JOINT EUROPEAN TORUS

JET–P(90)40

M.A. Kovanen, W.G.F. Core
and JET Team

HECTOR: A Code for the Study of Charged Particles in Axisymmetric Tokamak Plasmas

HECTOR: A Code for the Study of Charged Particles in Axisymmetric Tokamak Plasmas

M.A. Kovanen[1], W.G.F. Core
and JET Team*

JET-Joint Undertaking, Culham Science Centre, OX14 3DB, Abingdon, UK

[1]Lappeenranta University of Technology, Finland and National Research Council for Technology, The Academy of Finland
** See Appendix 1*

HECTOR: A Code for the Study of Charged Particles in Axisymmetric Tokamak Plasmas

M.A. Kovanen* and W.G.F. Core

JET Joint Undertaking, Abingdon, Oxon. OX14 3EA, UK

ABSTRACT

A new charged particle orbit following code HECTOR is described. The code simulates the behaviour of thermal particles, and high energy particles, such as those resulting from the ICRF wave field interactions or from thermonuclear reactions within the confining magnetic fields of non-circular axisymmetric tokamak plasmas. The particle trajectories are traced in the (C.O.M.) space using a new, fast, and efficient hybrid orbit following scheme based upon the drift equations in the guiding centre approximation and the constants of motion. The Monte-Carlo technique is used to describe the Coulomb scattering processes of dynamical friction, pitch angle scattering, energy diffusion, and ICRF interaction processes. The code is specifically designed to operate within the experimental environment.

I. INTRODUCTION

The operation of large tokamaks (JET, TFTR) with substantial levels of additional heating or close to ignition conditions leads to the occurrence of supra-thermal ion tails and of significant concentrations of fusion products within the plasma volume. These charged particles have energies in the MeV range, have long slowing down times which are typically 1 sec in systems close to ignition, have large Larmor radii and, especially for particles trapped in the toroidal field gradients, make large radial excursions across the minor cross-

---

* Lappeenranta University of Technology, Finland and National Research Council for Technology, The Academy of Finland

section of the torus. Large banana width particles will lead to a significant broadening of the heating profile, and in addition can be produced on orbits that intersect the vessel wall or enter the "loss cone" through particle-wave interactions or Coulomb scattering on the background plasma, leading to increased impurity production and wall loading. Furthermore, these escaping fast ions can provide important information on the auxiliary heating efficiency and thermonuclear activity within the discharge. A detailed knowledge of the orbit trajectories is essential to the theoretical and experimental understanding of tokamak systems close to ignition. The common use of small banana width approximations in these situations is highly questionable and may lead to serious erroneous results. An accurate description of the charged particle behaviour is therefore of primary importance for reactor feasibility studies and for diagnostic purposes.

A number of Monte Carlo codes or codes using the constant of motion (C.O.M.) method have been developed either to classify the orbit topology or to follow the guiding centre of charged particles moving in the magnetic field of a tokamak or similar plasma containment devices [1-16]. Many of the codes have only a limited number of applications, particularly those which relate to present day experiments. The most severe problem, however, is that the timescale to find the heating and diffusion rates is so long that the numerical uncertainties often dominate any perceived physics, or the demand for the computational resources is so large that such codes are far too expensive for routine use in the predictive or experimental environment. It is clear that there is a pressing need for a fast code which can be used to address a number of important charged particle problems.

In this work we describe a procedure for tracing charged particle orbits in non-circular tokamak containment systems. The code was originally designed to study the behaviour of fast ions residing in the tail of ICRF distributions or resulting from fusion reactions within the discharge. However, many

applications require an accurate description of the thermal particle behaviour, consequently, a treatment of low energy particles is also included in the code. The consideration is restricted to systems exhibiting toroidal axisymmetry and includes the Coulomb scattering processes of dynamical friction, pitch angle scattering, and energy diffusion due to collisions with the background electrons and ions, and the resonant ion interaction with ICRF wave fields. A hybrid integration scheme based upon the drift equations in the guiding centre approximation and the (C.O.M.) method is used to follow the test particles. In this numerical technique, the problem of error accumulation is avoided, the invariance of the toroidal canonical momentum enables arbitrarily large integration steps to be used, and particle trajectories obtained in this way remain close to the actual orbit throughout the integration.

The structure of this work is as follows. In Section II, the methods for the investigation of charged particle behaviour in the confining magnetic field of a tokamak plasma are reviewed and their areas of application discussed. In Section III, the Monte Carlo operators, describing the Coulomb collision and ICRF-wave interaction processes of ions moving in the confining field of a tokamak, are presented. Then in Section IV the procedure for mapping the charged particle source distribution from the local phase-space coordinates to the (C.O.M.) system is described. In Section V, the code input data specification and modes of operation are detailed, and finally in Section VI the test results are presented.

II. METHODS FOR THE INVESTIGATION OF CHARGED PARTICLE TRAJECTORIES

In this section we first review current methods and areas of application for tracking charged particles in tokamak containment systems. Then a new method based upon the drift equations in the guiding centre approximation and the constants of motion is described. The coordinate system used is shown in Fig. 1.

(i) **Full Orbit Calculation**

The full equation of motion for charged particles is:

$$m\vec{v} = q\left(\vec{E} + \vec{v} \times \vec{B}\right)$$

where m is the particle mass, v is the particle velocity, q is the particle charge, and E,B are the electric and magnetic field strengths, respectively. This equation is solved in HECTOR with a 2-step predictor-corrector method.

The advantage of using the exact equation is its accuracy in describing the orbits. However, calculations of this type besides having error accumulation are time consuming and not well suited to simulation studies where a large number of particle trajectories are to be examined. Consequently, the full orbit representation is limited to situations where detailed information on the actual particle trajectory is required, such as orbits for heavy ions with low charge state.

(ii) **Guiding Centre Approximation**

From the collisionless drift equations the velocity components of the guiding centre are readily obtained, we have:

$$\vec{v}_{g.c.} = v_{\parallel}\vec{b} - v_{\parallel}\vec{b} \times \nabla\left(\frac{v_{\parallel}}{\omega_{ci}}\right)$$

where the component of the guiding centre velocity projected along the magnetic field line is $v_{\parallel} = \pm [2(E - \mu B/m)]^{1/2}$, $\vec{b} = \vec{B}/|\vec{B}|$ is the unit vector in the direction of the magnetic field, $\omega_{ci} = qB/m$ is the ion cyclotron frequency, $E = \frac{1}{2} mv^2$ is the particle energy, $\mu = \frac{1}{2} mv_{\perp}^2/B$ is the magnetic momentum, and $v, v_{\perp}$ are the magnitude and perpendicular components of the particle velocity, respectively. The numerical integration is done using the modified Euler second order predictor-corrector method [17].

Whatever numerical integration method is used for the guiding centre equation, there are two severe problems. The first is the accumulative

numerical error which limits the integration step length to 10-20 times the step length used with full orbit calculations. In order to be able to simulate thousands of slowing down orbits, a greatly enhanced numerical acceleration (>10^3) of the slowing down processes must be introduced leading to a distorted orbit topology. The effect of the accumulative numerical error on a typical orbit is shown in Fig. 2. It is to be noted that the error in flux coordinate appears to grow almost linearly with integrated orbit trajectory. The second problem is the turning point, where $v_{\|}$ changes sign. In order to implement the long integration step procedure the actual coordinates of the orbit turning point coordinates, where ($v_{\|}$ = 0), can require a considerable investment in interpolation, and consequently, a significant fraction of the computational time. In the following section, a method of orbit integration is described which surmounts these difficulties.

(iii) Drift Equation and Constants of Motion Approximation (C.O.M.) Hybrid-Method

In the absence of interacting processes three constants of motion, the particle velocity v, magnetic momentum μ and toroidal canonical angular momentum P_ϕ completely characterise the guiding centre motion of charged particles moving within the confining magnetic fields of a axisymmetric tokamak. In systems having arbitrary cross section [18]

$$P_\phi = mR\, v_{\|} B_\phi / B - q\psi$$

where $B^2 = B_R^2 + B_\phi^2 + B_Z^2$, and ψ is the poloidal flux function.

If a simple formula for ψ is used, the spatial coordinates of the charged particle can easily be solved. This, however, represents only a small minority of cases relevant to present day tokamaks. In the general situation ψ is obtained either as a numerical solution of the Grad-Shafranov equation for plasma equilibria, or as a fit to the experimental magnetic measurements. Thus, an alternative method to find the spatial coordinates has to be used. This is usually done by writing the set of (P_ϕ,μ,v) invariants as a function of R and ψ, and by

assuming $B = B_\phi$ [16]. The (R,Z)-coordinates can then be obtained by a 1-dimensional interpolation of ψ. The resulting error in orbit topology when compared with the case where the poloidal magnetic finite component B_θ is included is small if the plasma current is low [19], but will become significant for current values used in the present large tokamaks currently operating (JET,TFTR) or in future igniting tokamaks.

To include B_θ the interpolation has to be done in 2-dimensional (R,ψ) space. This is done in HECTOR with a hybrid integration technique which combines the drift equations and the (C.O.M.) method. First, a long single guiding centre step is taken to give predicted spatial coordinates. The coordinates are then corrected by linear interpolation to find the actual coordinates that satisfy P_ϕ = constant. The drift equation gives the optimum predicted spatial coordinates, and consequently, increases the overall efficiency of the integration procedure. The sign of $v_\parallel$ is automatically included in the integration, numerical error accumulation, and the problem of locating the spatial coordinates of the turning points are avoided. With this method the integration step length can be up to two orders of magnitude longer than the step length used to solve the drift equations using standard corrector-predictor methods. This enables the slowing down enhancement factor to be significantly reduced and, thus, the orbit degradation that occurs in other integration schemes is avoided. An example of a first orbit using long integration steps is shown in Fig. 3.

III. SLOWING DOWN AND ICRF-INTERACTION PROCEDURE

The inclusion of the effects of Coulomb scattering and ICRF-interaction on the particle trajectories is straightforward and conceptually simple. Collisions are taken into account by calculating new values of particle velocity, the magnetic momentum, and the toroidal canonical angular momentum after each time step. We have

$$v \rightarrow v + \Delta v$$

$$\mu \rightarrow \mu + \Delta\mu$$

$$P_\phi \rightarrow P_\phi + \Delta P_\phi ,$$

where

$$\Delta\mu = \frac{m}{2B}\left(2v\Delta v + \Delta v^2 - 2v_\parallel \Delta v_\parallel - \Delta v_\parallel^2\right),$$

and

$$\Delta P_\phi = m R B_\phi \Delta v_\parallel / B,$$

are the incremental changes in magnetic moment ($\Delta\mu$), and toroidal canonical momentum (ΔP_ϕ) due to the accumulative effects of dynamical friction, pitch angle scattering, energy diffusion, and rf-wave interaction occurring during the time step. Δv, and $\Delta v_\parallel$ are the incremental changes in particle velocity and it's parallel component, respectively.The above set of equations have the important feature of energy conservation.

(i) **Friction**

Following the analytical treatment of the Fokker-Planck equation by Stix, one can write the change in particle velocity occurring during a time interval Δt [20].

$$\Delta v = -\sum_f \left(C_f \frac{m}{2kT_f} G\left(\ell_f v\right)\Delta t \right),$$

where

$$C_f = 8\pi n_f Z_f^2 Z^2 e^4 \ell n\Lambda / m^2$$

$$\ell_f{}^2 = m_f / \left(2kT_f\right)$$

$$G(x) = \frac{\phi(x) - x\phi'(x)}{2x^2}$$

$$\phi(x) = \frac{2}{\pi^{1/2}} \int_o^x e^{-y^2} dy$$

and the subscript f designates the background field particles, ions and electrons. The change in the parallel velocity due to this change in velocity Δv is then given by

$$\Delta v_{\|} = \xi \Delta v,$$

where ξ is the pitch, the cosine of the pitch angle. Fig. 4 shows the effect of friction on a 1 MeV triton slowing down orbit.

(ii) **Pitch Angle Scattering**

Boozer and Kuo-Petravic have derived a simple Monte-Carlo equivalent Lorentz collision operator based on a binomial distribution [22]. The change in the parallel velocity during Δt is

$$\Delta v_{\|} = v \Delta \xi,$$

where

$$\Delta \xi = \nu \Delta t \xi + \delta_1 \left[\left(1 - \xi^2\right) \nu \Delta t \right]^{1/2}.$$

δ_1 is $\pm$ 1 with equal probabilities and the collision frequency ν given by Spitzer [21], is

$$\nu = \frac{1}{2v^3} \sum_f C_f \left[\phi\left(\ell_f v\right) - G\left(\ell_f v\right) \right].$$

Fig. 5 demonstrates the combined effects of pitch angle scattering and friction on a 1 MeV triton slowing down orbit.

(iii) **Energy Scattering**

Boozer and Kuo-Petravic have also given an energy scattering equivalent of the Lorentz scattering operator [22]. The change in particle energy during Δt is

$$\Delta E = -2 v_E \Delta t \left[E - \left(\frac{3}{2} + \frac{E}{v_E} \frac{dv_E}{dE} \right) T \right] + \delta_2 \left[4TE (v_E \Delta t) \right]^{1/2},$$

where δ_2 is $\pm$ 1 with equal probabilities, and T is the background Maxwellian temperature. The energy scattering frequency is [21]

$$\nu_E = \frac{1}{v^3}\sum_f \left[C_f G(\ell_f v)(\ell_f v)^2 \right].$$

The change in particle velocity is then

$$\Delta v = \left[v^2 + \frac{2}{m}\Delta E \right]^{1/2} - v,$$

and the corresponding change in the parallel velocity is

$$\Delta v_\parallel = \xi \Delta v.$$

Fig. 6 shows a 1 MeV triton slowing down orbit where in addition to friction and pitch angle scattering, energy diffusion is also included.

(iv) **ICRF Interaction**

Each time the ion passes through the ion cyclotron resonance layer and undergoes resonant interaction with the wave field there is a random change in the perpendicular component of the particle velocity. This incremental charge in velocity can be readily obtained by integrating the equations of motion over the unperturbed particle trajectories [20] and is given by:

$$\Delta v_\perp = \frac{q}{m}\left(\frac{2\pi}{|\dot{\Omega}|}\right)^{1/2} |E_+| e^{-LZ^2} g(Z) \cos\alpha \left[J_{n-1}\left(\frac{k_\perp v_\perp}{\omega_{ci}}\right) + \frac{E_-}{E_+} J_{n+1}\left(\frac{k_\perp v_\perp}{\omega_{ci}}\right) \right],$$

where E is the electric field strength with + and - designating the polarized left- and right-handed components, respectively. L is the electric field profile parameter, Z is the distance from the median plane in the vertical direction, and α is the phase angle. g(Z) is a function which is used to provide a flat power absorption profile when L = 0. J_n is the usual Bessel function of order n and $k_\perp$ is the perpendicular wave number. The time variation of the cyclotron frequency seen by the drifting ion as it passes through the resonance layer is

$$\dot{\Omega} = \frac{v_\parallel \Omega_{ci} B_\theta}{B_\phi R}\sin\theta,$$

and

$$\alpha = 2\pi\delta_3,$$

where δ_3 is a uniformly distributed random number between 0 and 1. The change in the particle velocity is then obtained from

$$\Delta v = \left[v^2 + 2\left(v^2 - v_{\parallel}^2\right)^{1/2} \Delta v_{\perp} + \Delta v_{\perp}^2 \right]^{1/2} - v$$

The rf-induced diffusion is taken into account by calculating the change in the parallel velocity component [20]:

$$\Delta v_{\parallel} = k_{\parallel} v_{\perp} \Delta v_{\perp} / \Omega_{ci},$$

where $k_{\parallel}$ is the parallel wave number. In Fig. 7 we show a typical guiding centre orbit of an ICRF heated ^{3}He ion in deuterium plasma.

(v) **Acceleration of Scattering processes**

Following charged particle trajectories is time consuming, thus, to achieve acceptable computing time an enhanced acceleration of the slowing down and scattering processes has to be introduced. Goldston et al. coupled the acceleration to the change in pitch $|\Delta\xi|$ with a predetermined acceleration constant G [10]. The acceleration was reduced by a factor of 2 when the change in pitch is above the upper limit G and increased by the same factor below the lower limit $\sqrt{0.5}$ G. To improve statistics in HECTOR the increase/decrease factor of 1.3, and the lower limit of 0.5 G are used. Typically G can be 0.05 - 0.08, but higher values will lead to increased scattering losses due to enhanced change from passing orbits to trapped ones.

When velocity increases the reduction in the scattering frequency occurs at a faster rate than in the timestep $\Delta t = \Delta s/v$, where Δs is a constant spatial step. Thus, to prevent an excessive growth in acceleration, which would lead to a distorted slowing down and tail formation during ICRH, an upper limit for the acceleration is required. A fixed value upper limit is not efficient in view of CPU time, and thus, a scaling factor $(v/v_{th})^{1/2}$ is added during slowing down calculations. When the ICRH is on, to improve the statistics near the axis where

the particle-wave field is the strongest, the acceleration is in addition multiplied with $\left[1+a\left(1-e^{-LZ^2}\right)\right]$.. Typically acceleration of the order of 20 and the constant a value of 2 are used.

IV. SOURCE FUNCTION FOR CHARGED PARTICLES AND YIELD CALCULATION

In this section we consider the problem of source definition. The application of direct sampling methods to the problem of particle selection from the distribution of sources in the local phase-space coordinates leads to orbit duplication and many repetitions of the same equivalent particle occurs. Consequently, a very large number of particles will have to be tracked in order to obtain reasonable statistical accuracy. In order to circumvent this difficulty, we note that particles produced in different regions of phase space are simply connected through a unique set of (P = P_ϕ,μ,v) coordinates (Fig. 8) and that all particles produced on a particular orbit connecting different regions of phase space are equivalent. It is clear that the path of a representative particle will be determined by the initial values of (P,μ,v). The point on the path at which these initial values are specified is usually taken to be the median plane of the torus, but is otherwise quite arbitrary. In this way, a transformation to the (C.O.M.) space will lead to a significant reduction in the number of charged particles that have to be tracked to ensure that sampling errors are minimised. The charged particles bounce averaged source in the local velocity-space variables (R,Z,v,ξ) is transferred to the C.O.M. system (P,μ,v), where the local source strength is given by

$$S = 4\pi^2 \int\int\int\int S(R,Z,\mathrm{v},\xi) R dR dZ \mathrm{v}^2 d\mathrm{v} d\xi.$$

For charged particles resulting from thermonuclear reactions within the plasma the local source function takes the following form

$$S(R,Z,\mathrm{v},\xi) = \frac{n_1 n_2 < \sigma \mathrm{v} >}{4\pi \mathrm{v}_0^2} \cdot \delta(\mathrm{v} - \mathrm{v}_0),$$

where $<\sigma v>$ is the thermonuclear reactivity, v_o is the birth velocity, and the particles are assumed to be born isotropically in velocity space. The local birth rate of fast neutral beam particles is described with

$$\dot{n} = (\dot{n}_o - \dot{n}_e)(1 - x^a)^b + \dot{n}_e,$$

where the subscripts (o,e) refer to the values on the magnetic axes, and at the plasma edge, respectively, and (a,b) are the profile parameters. The initial pitch is assumed to have a narrow gaussian distribution, and is related to the major radius by

$$\xi = \xi_e \left(\frac{R_e}{R} \right)^c,$$

where c is a factor determined by the beam line geometry.

The starting point of each test particle, in the (P,μ,v) grid, is mapped onto the median plane of the torus, and the weight factor for each flight is set equal to the corresponding bounce averaged source rate.

Thermonuclear yields are calculated by integrating the hot target reactivity $<\sigma v>_h$ [23] along the particle orbits, and the burn-up fraction is calculated from

$$\rho = \frac{\sum_k N_{o_k} \left[1 - \pi (1 - < \sigma v >_h n \Delta t)_i \right]}{\sum_k N_{o_k}}$$

where N_{ok} is the number of test particles born, and n is the target density. Index i refers to the integration steps along the orbit.

V. INPUT DATA

Tracing the charged particles requires a continuous supply of local values of magnetic field and bulk plasma parameters along the orbit trajectory. Two equidistant (but not limited to) spatial grids are used to facilitate an easy access to these values.

The radial density and temperature profiles of plasma electrons, primary ions and impurity ions, and the calculated profiles of thermonuclear reactivities,

and other cross-sections of interest such as charge-exchange are stored in 51 grid points. The values of the magnetic field components B_R, B_ϕ, B_Z, the magnitude of the field $|\vec{B}|$, the flux coordinate ρ, poloidal flux function ψ, and the reference coordinates of the 1-D grid are pre-calculated and stored in a 2-D grid spanning the entire poloidal cross section of the torus. To obtain particular values and reduce the computational time still further and furthermore, avoid recourse to interpolation we employ a simple table "look-up" procedure. Unfortunately, this procedure demands a fine grid, resulting in a considerable increase in storage requirements. However, a (200 × 299) grid was found to give acceptable results. Input data can be divided into two categories depending on whether arbitrary values and profiles (arbitrary input data) or data from JET shots (JET shot input data) are used.

(i) **Arbitrary Input Data**

In this mode the code can be used with a wide variety of input parameters appropriate to other tokamaks in addition to JET.

The built-in profiles for electron and ion densities and temperatures are:

$$n_j = \left(n_{jo} - n_{je}\right)\left(1 - x^2\right)^a + n_{je}$$

$$T_j = \left(T_{jo} - T_{je}\right)\left(1 - x^2\right)^b + T_{je} \quad , j = (i,e)$$

The constants a,b and c are the usual profile parameters.

The toroidal component of the magnetic field is calculated from:

$$B_\phi = B_o R_o / R$$

where B_o, is the toroidal magnetic field at $R = R_o$.

The poloidal magnetic field, B_θ is derived from the Lao-Hirshman solution of the Grad-Shafranov equation for plasma equilibria and assumes an analytical representation for the plasma current and pressure profiles [24] which has been corrected to satisfy $\nabla \cdot \vec{B} = 0$ [23]. Both symmetric and non-symmetric plasma cross sections can be included. The input parameters for the B_θ

calculations are: plasma current, current profile constant, beta-i, elongation, internal inductance and minor radius. As the output, poloidal field components and the flux coordinate are returned. In the hybrid method the value of the poloidal flux ψ is needed, and this is obtained by integrating over the median plane the equation,

$$\frac{\partial \psi}{\partial R} = B_\theta R.$$

(ii) JET Shot Input Data

To obtain the poloidal flux function ψ the code IDENTC is used [25]. The code solves the Grad-Shafranov equation for plasma equilibria assuming an analytical representation of the current and pressure profiles and using free parameters to fit the data from the magnetic measurements. The output is a normalized ψ between 0 and 1.

The FLUSH routine package [26] is then used to calculate the actual values of ψ, and the poloidal magnetic field components B_R, B_z, at given coordinates.

Routine PREGER [27] is used to extract data, such as n_e, T_e profiles, from JET shot data banks. Densities for the primary ions and the impurities are then calculated using the impurity routine CPRIO [27], which employs the coronal equilibrium model. The local birth rate of fast neutral beam particles can be included by fitting the data from the PENCIL code [28].

VI. TEST RESULTS

An extensive program of tests was carried out to assess the reliability and accuracy of HECTOR. The comparison with the SOCRATE code [16], which combines the single orbit approximation with the classical energy loss formula, showed a very good agreement in the orbit topology, the source rate, the slowing down rate, and the triton burn-up (Table 1) [19].

The spread in pitch for a single thermal ^{3}He-particle behaved as expected, and in the JET deuterium plasma reached a uniform distribution after several collision times (Fig. 9). Furthermore, the diffusion coefficient, and the consequent particle losses were within 10% of the neoclassical values.

Separate tests of the energy diffusion operator showed, that the relaxation of a thermal ^{3}He-particle in energy space reached the Maxwellian distribution in a timescale longer than for the pitch relaxation (Fig. 10).

The validity of the ICRF interaction model was tested by comparing it with a semi-analytical model [29] which is in good agreement with the bounce averaged Fokker-Planck ion cyclotron code BAFIC [30]. Flat profiles for the rf wave fields and plasma parameters enabled to eliminate the finite orbit effects in the results obtained using HECTOR. The minority ion energy content, the mean energy (Fig. 14), the energy transferred to background electrons and ions (Fig. 12), and the fusion yield (Fig. 13) are in good agreement, within 10%, when particle losses in HECTOR are taken into account.

VII. CONCLUDING REMARKS

The new numerical techniques for tracing orbits together with a fine 2-D spatial grid combined with its corresponding 1-D grid, have reduced the computation time for each particle flight. Introducing the bounce averaged source rate has reduced significantly the number of particle orbits that have to be tracked. A simulation following 2000 test particles for a Spitzer time takes only 15-20 min CPU time on the IBM-3090-300J.

The time evolution of the plasma parameters can be taken into account during the slowing down but the increasing CPU time and space requirement reduces the number of time grid points to 5-10. In most applications the assumption of the steady state plasma is sufficient.

Acknowledgements

We wish to thank the following members of the JET Theory Division. A. Taroni, C. Sack and E. Springmann for providing program modules TRESCO, DBGET, PREGER, CPRIO, FLUSH and FLUPNG for the JET short data input mode, and P. van Belle and G. Sadler for providing program modules for full orbit calculations including the poloidal field presentation for the arbitrary input mode, and the routine for the hot target reactivity. We also appreciate fruitful discussions with H. Hamnén and T. Hellsten. Help from the JET Data Management Group is appreciated, and we also wish to thank Mrs S. Costar for typing the text so carefully.

M.A. Kovanen is grateful to JET Theory Division for hospitality, and to the Finnish Cultural Foundation, and to Jenny and Antti Wihuri's Foundation for financial support.

References

[1] DEI-CAS, R., MARTY, D., Fontenay-aux-Roses Rep. EUR-CEA-FC-726 (1974).

[2] OHNISHI, M., TOKUNAGA, J., WAKABAYASHI, J., Nucl. Fusion 16 (1976), p. 693

[3] JASSBY, D.L., GOLDSTON, R.J., Nucl. Fusion 16 (1976), p.613.

[4] LISTER, G.G.G., POST, D.E., GOLDSTON, R.J., in 3rd Varenna Symposium on Plasma Heating in Toroidal Devices (Editrice Compositori, Bologna, Italy, 1976), p. 303.

[5] PETRIE, T.W., MILEY, G.H., Nucl. Sci. Eng. 64 (1977), p. 151.

[6] OHNISHI, M., AO, N., WAKABAYASHI, J., Nucl. Fusion 18 (1978), p. 859.

[7] BAUER, W., WILSON, K.L., BISSON, C.L., HAGGMARK, L.G., GOLDSTON, R.J., Nucl. Fusion 19 (1979), p. 93.

[8] MIKKELSEN, D.R., POST, D.E., in Theoretical Aspects of Controlled Thermonuclear Fusion (Proc. Sherwood Conf. Mt. Pocono, 1979), Paper 1B21.

[9] FOWLER, R.H., ROME, J.A., Oak Ridge National Lab. Rep. ORNL/TM-7774 (1981).

[10] GOLDSTON, R.J., McCUNE, D.C., TOWNER, H.H., DAVIS, S.L., HAWRYLUK, R.J., SCHMIDT, G.L., J. Comput. Phys. 43 (1981), p. 61.

[11] GAGEY, B., LAPIERRE, Y., MARTY, D., in 3rd Joint Varenna-Grenoble Int. Symposium on Heating in Toroidal Plasmas (Centre D'Etudes Nucleaires de Grenoble, France, 1982), p. 361.

[12] TANI, K., TAKIZUKA, T., AZUMI, M., KISHIMOTO, H., Nucl. Fusion 23 (1983), p. 657.

[13] WHANG, K.W., MORALES, G.J., Nucl. Fusion 23 (1983), 481.

[14] HIVELY, L.M., Nucl. Fusion 24 (1984), p. 779.

[15] LISTER, G.G., IPP 4/222, Max-Planck-Institut für Plasma physik (1985).

[16] BITTONI, E., HAEGI, M., RT-FUS-86-13, Ass. EURATOM ENEA Sulla Fusione CRE-FRASCATI (Roma).

[17] HAMMING, R.W., Introduction to Applied Numerical Analysis, McGraw-Hill, Inc., 1971.

[18] HIVELY, L.M., MILEY, G.H. and ROME, J.A., Nuclear Fusion, Vol. 21, No. 11 (1981), p. 1431.

[19] GORINI, G. and KOVANEN, M.A., JET Joint Undertaking, JET-R(88)09.

[20] STIX, T.H., Nuclear Fusion 15 (1975), p. 737.

[21] SPITZER, L. Jr., The Physics of Fully Ionized Gases, 2nd Revised Ed., Interscience, New York (1962).

[22] BOOZER, A.H. and KUO-PETRAVIC, G., Phys. Fluids 24, (1981), p. 851.

[23] Van BELLE, P. and SADLER, G., Private communications.

[24] STRINGER, T.E., JET Joint Undertaking, JDN/T(83)6.

[25] LAZZARO, E. and MANTICA, P., Plasma Phys. and Contr. Fusion 30 (1988), p. 1735.

[26] SPRINGMANN, E.M., Private communications.

[27] SACK, H.C. and SPRINGMANN, E.M., Private communications.

[28] STUBBERFIELD, P.M. and WATKINS, M.L., JET Joint Undertaking, DPA(06)/87.

[29] ANDERSON, D., CORE, W.G.F., ERIKSSON, L.-G., HAMNÉN, H., HELLSTEN, T. and LISAK, M., Nucl. Fusion 27 (1987), p. 911.

[30] SUCCI, S., APPERT, K., CORE, W., HAMNÉN, H., HELLSTEN, T. and VACLAVIK, J., Comp. Phys. Comm. 40 (1986), p. 137.

TABLE 1

Triton burn-up and confined fraction calculated with HECTOR and SOCRATE codes. The effects of pitch angle scattering and energy diffusion are not included

	Shot: 10583				Shot: 10952			
	flat profile		peaked profile		flat profile		peaked profile	
	HECTOR	SOCRATE	HECTOR	SOCRATE	HECTOR	SOCRATE	HECTOR	SOCRATE
$\rho(\%)$	0.50	0.50	0.74	0.79	1.29	1.31	1.54	1.62
$f_C(\%)$	50	49	93	94	70	69	100	100

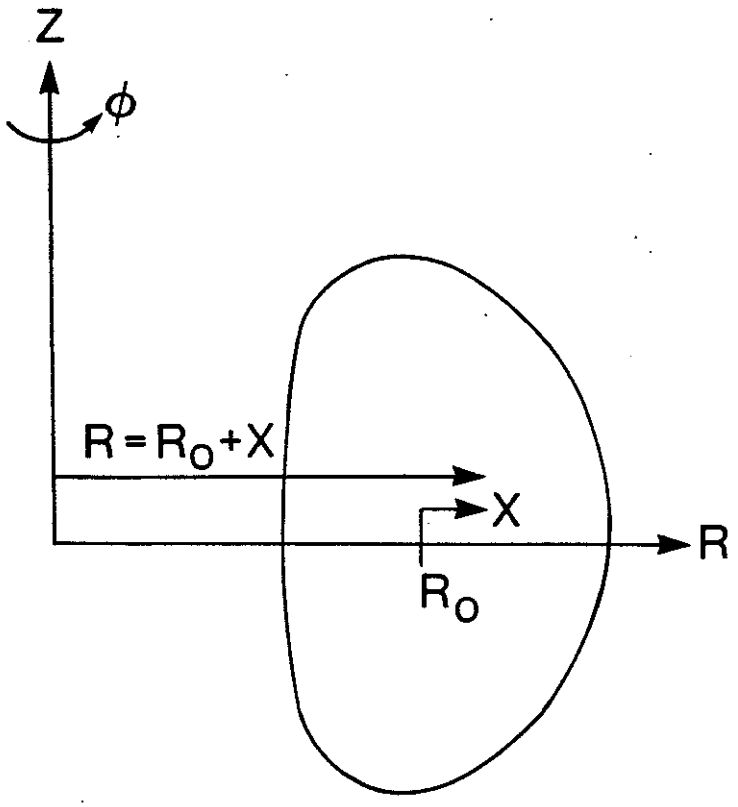

1. (R,ϕ,Z) - coordinate system.

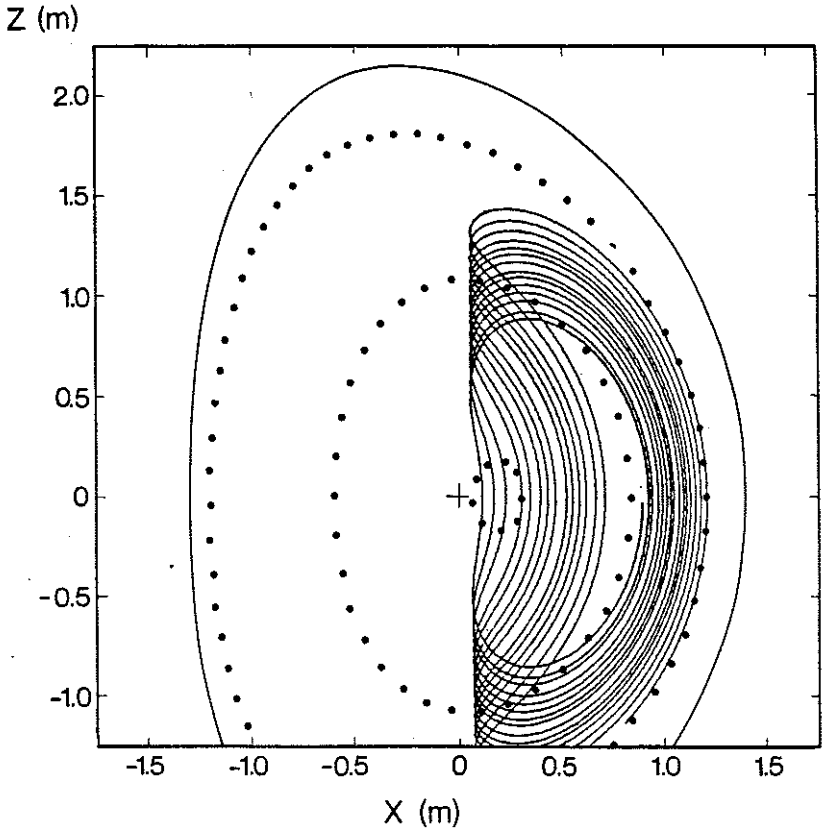

2. This figure shows the effect of the accumulative numerical error on a collisionless α-particle orbit calculated using the guiding centre approximation.

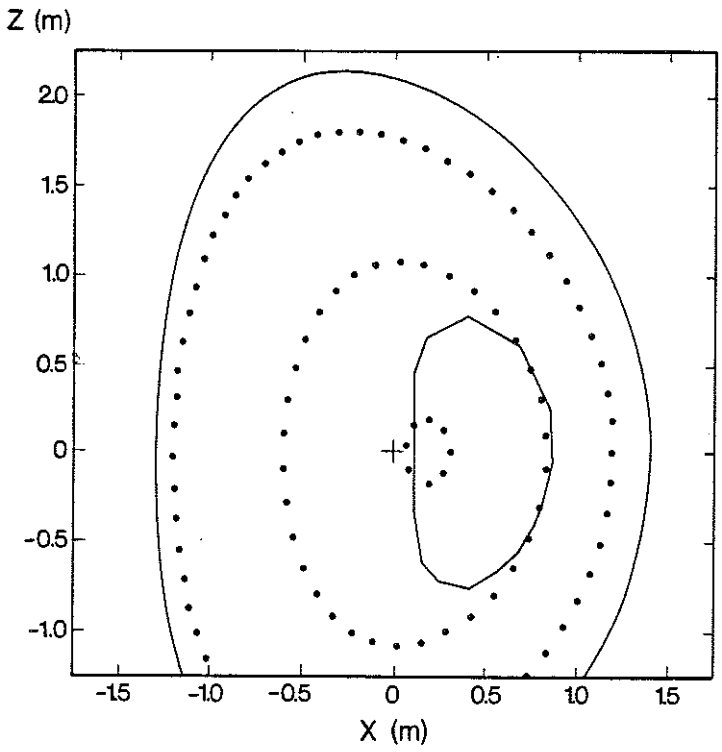

3. Here is shown a typical collisionless orbit traced using long (4 m) integration steps with the (C.O.M.) hybrid method. It is seen that even with this large integration step, the orbit remains closed.

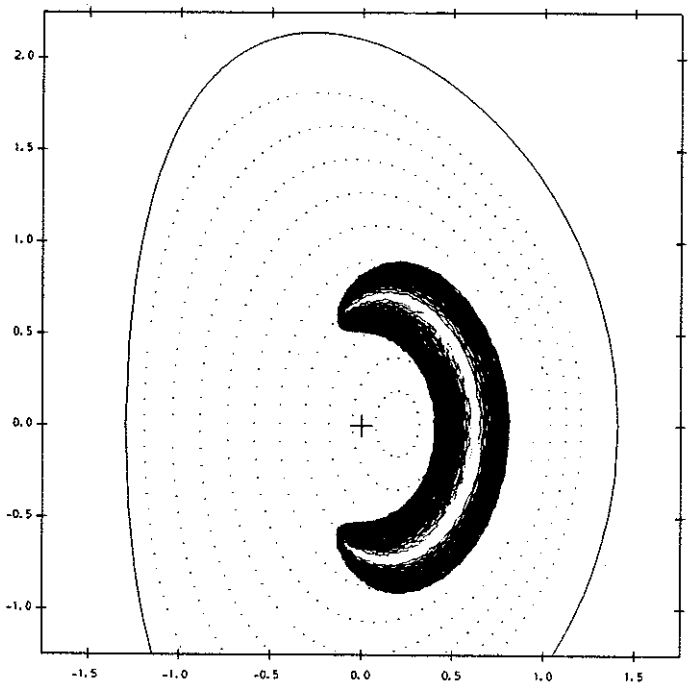

4. The slowing down orbit for a 1 MeV triton is shown. Only friction is included. The parameters for the calculation are I_p = 5 MA, B_ϕ = 3.4 T, T_e = 8 keV, $n_e = 5 \times 10^{19} m^{-3}$, Z_{eff} = 1.2, and initially the particle started at (X_o, Z_o, ξ_o) = (0.4, 0.0, -0.40). A smoother orbit would be obtained with shorter integration steps.

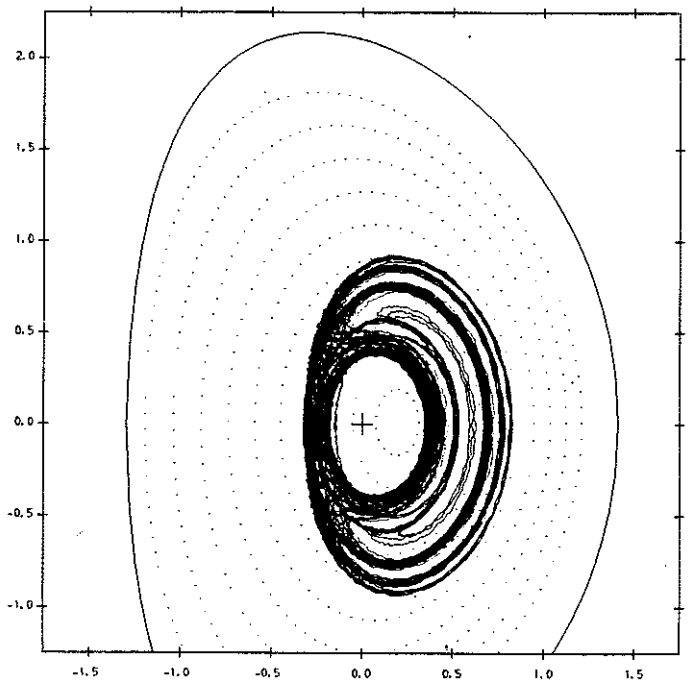

5. The slowing down orbit for a 1 MeV triton is shown. Both friction and pitch angle scattering are included. The parameters for the calculation are I_p = 5 MA. B_ϕ = 3.4 T, T_e = 8 keV, $n_e = 5 \times 10^{19} m^{-3}$, Z_{eff} = 1.2, and initially the particle started at (X_o, Z_o, ξ_o) = (0.4, 0.0, -0.40).

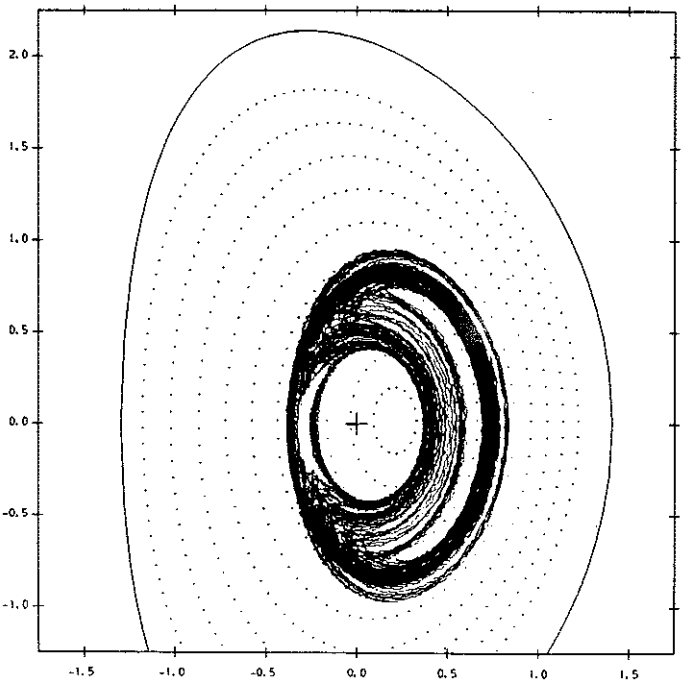

6. The slowing down orbit for a 1 MeV triton is shown. Friction, pitch angle scattering, and energy diffusion are included. The parameters for the calculation are I_p = 5 MA. B_ϕ = 3.4 T, T_e = 8 keV, $n_e = 5 \times 10^{19} m^{-3}$, Z_{eff} = 1.2, and initially the particle started at (X_o, Z_o, ξ_o) = (0.4, 0.0, -0.4).

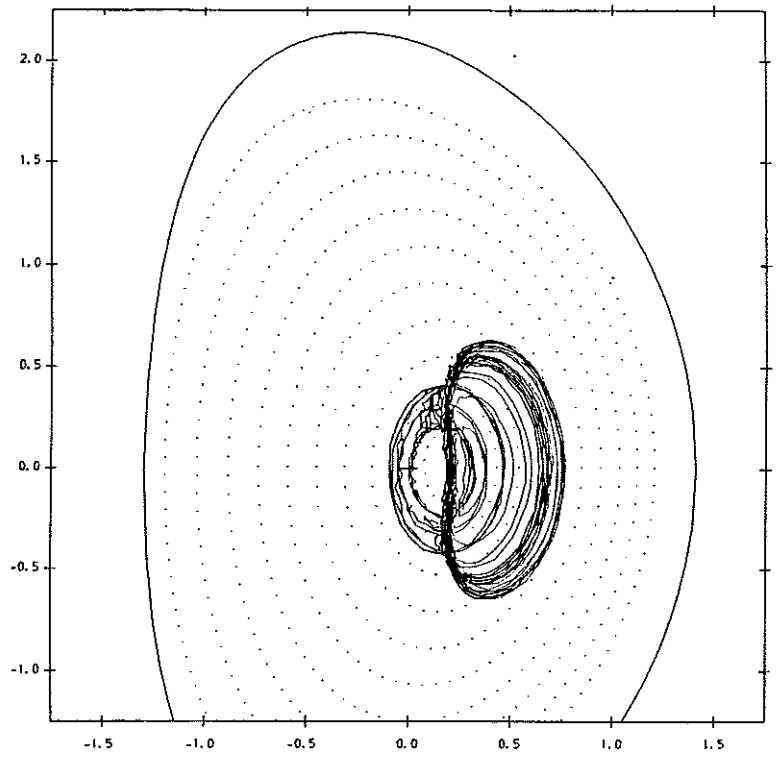

7. The orbit of a ICRF heated minority ^{3}He ion is shown. The calculation includes friction, pitch angle scattering, energy diffusion, and rf-wave interaction. The parameters are I_p = 5 MA. B_ϕ = 3.4 T, T_e = 8 keV, $n_e = 5 \times 10^{19} m^{-3}$, Z_{eff} = 1.2, and initially the particle started at (X_o, Z_o, ξ_o) = (0.4, 0.0, -0.4). The particle energy was initially T_e, and after Spitzer time it reached MeV range.

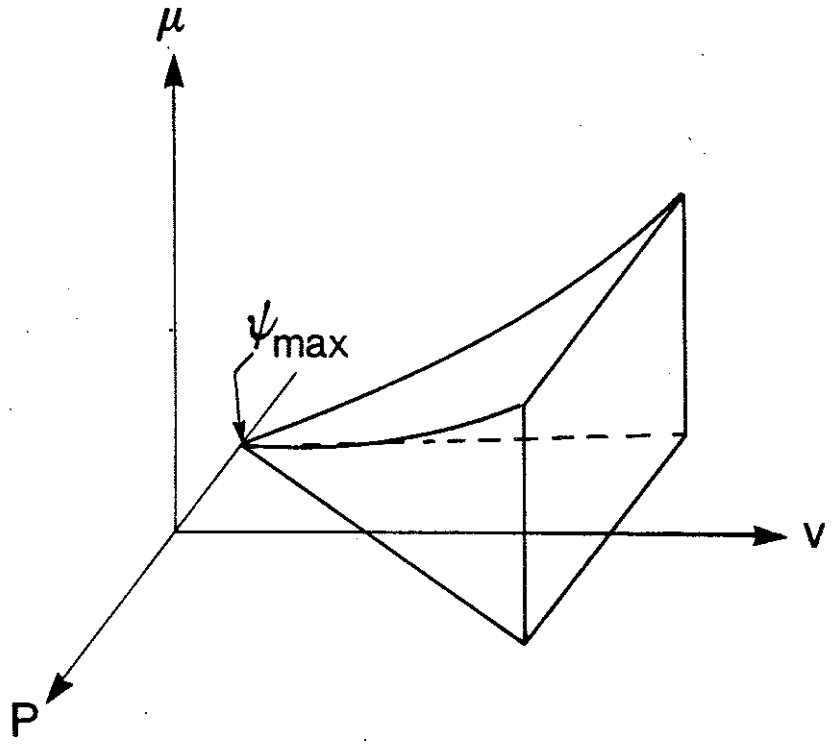

8. The geometry of the (P,μ,v)-source grid.

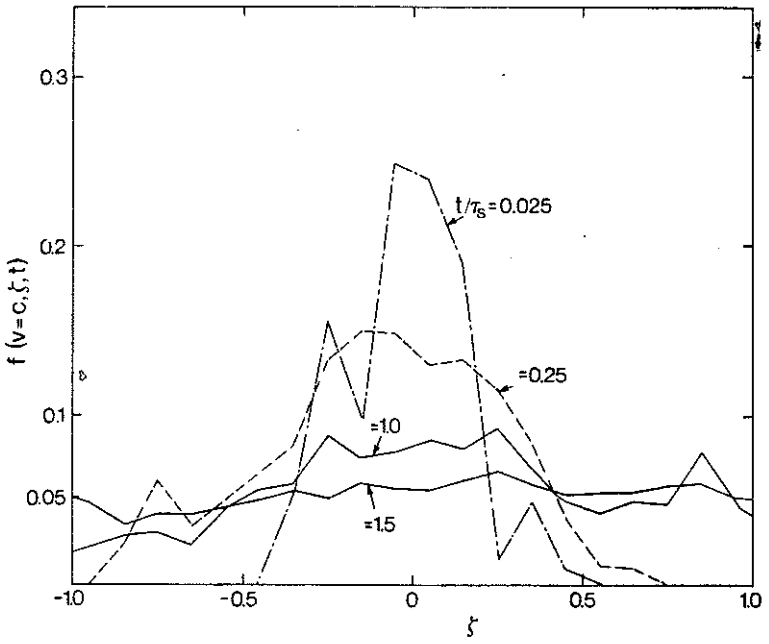

9. The particle relaxation in pitch space is shown. A single, thermal E = T, ^{3}He ion was followed with the pitch angle scattering operator in D plasma. The particle started with an initial pitch $\xi = 0.0$, and after 1.5 Spitzer time isotropic pitch distribution was obtained.

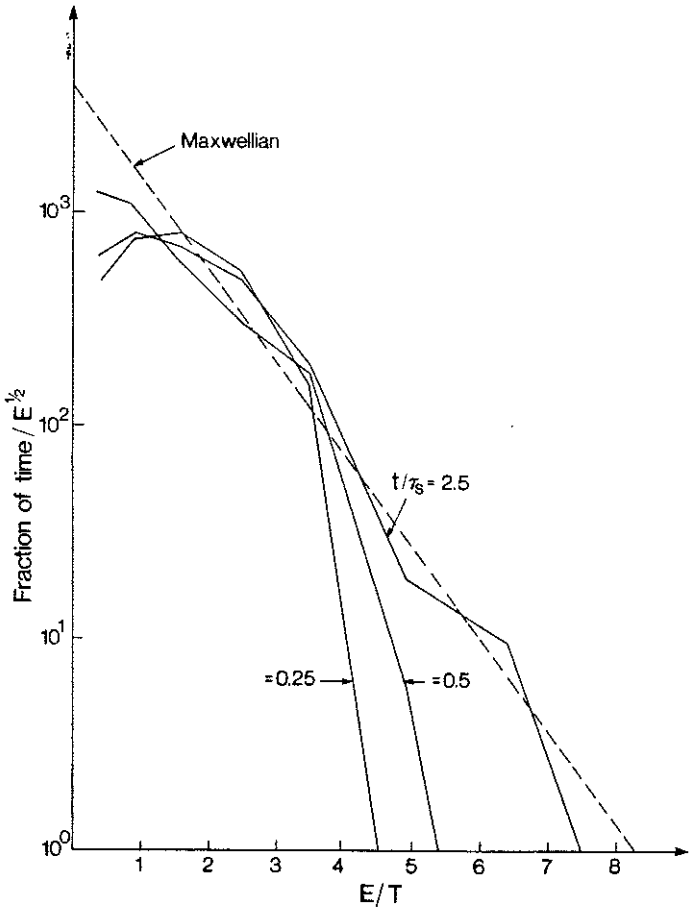

10. The particle relaxation in energy space is shown. A ^{3}He ion was followed with the energy scattering operator in D plasma. The initial energy was E = T. A Maxwellian distribution, represented with the straight line, is reached after 2.5 Spitzer time.

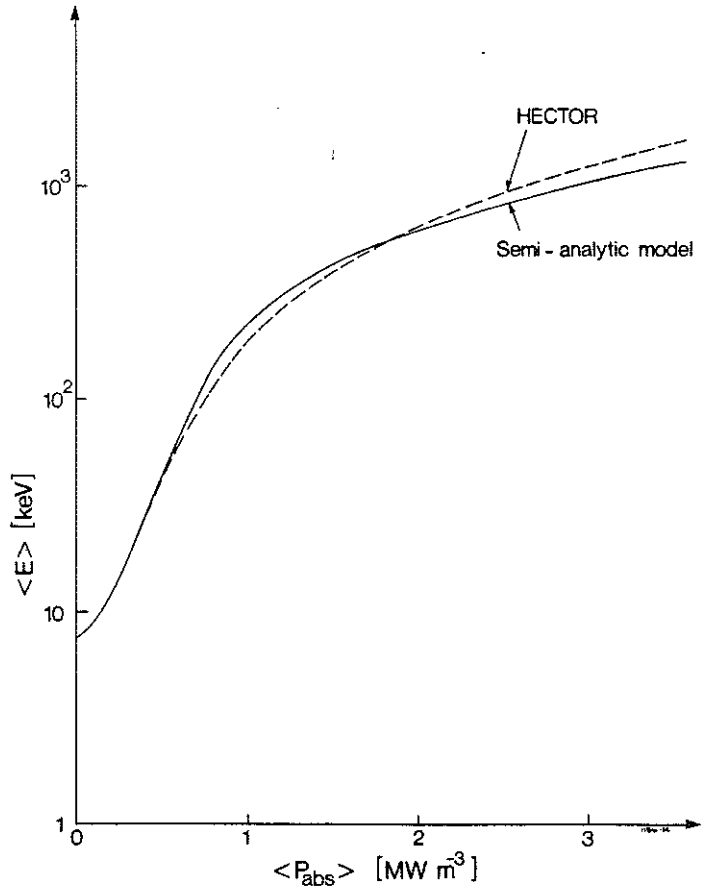

11. Comparison of the mean energy calculated with the Fokker-Planck and HECTOR codes. The parameters for the calculation are I_p = 5 MA. B_ϕ = 3.4 T, T_e = 8 keV, $n_e = 5 \times 10^{19} m^{-3}$, Z_{eff} = 1.2.

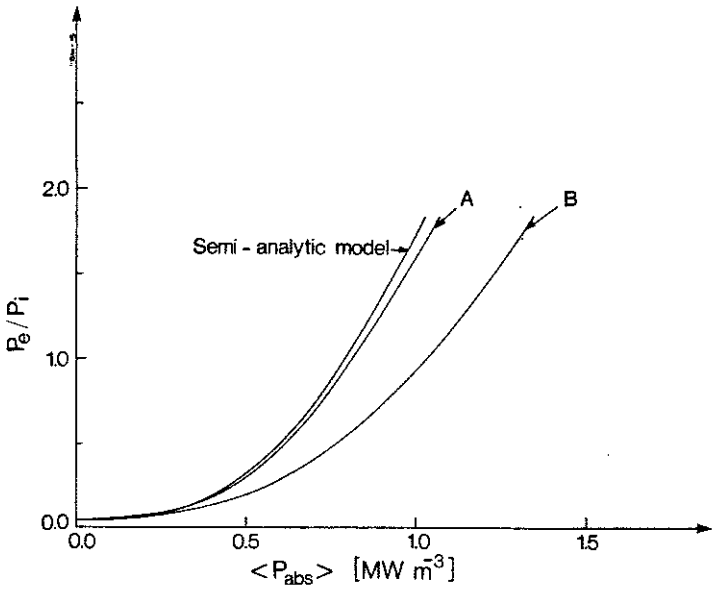

12. Comparison of the electron and background ion heating rates calculated with the Fokker-Planck and HECTOR codes. In case A the effect of the particle losses out of the plasma is not included but in case B it is. The parameters for the calculation are I_p = 5 MA. B_ϕ = 3.4 T, T_e = 8 keV, $n_e = 5 \times 10^{19} m^{-3}$, Z_{eff} = 1.2.

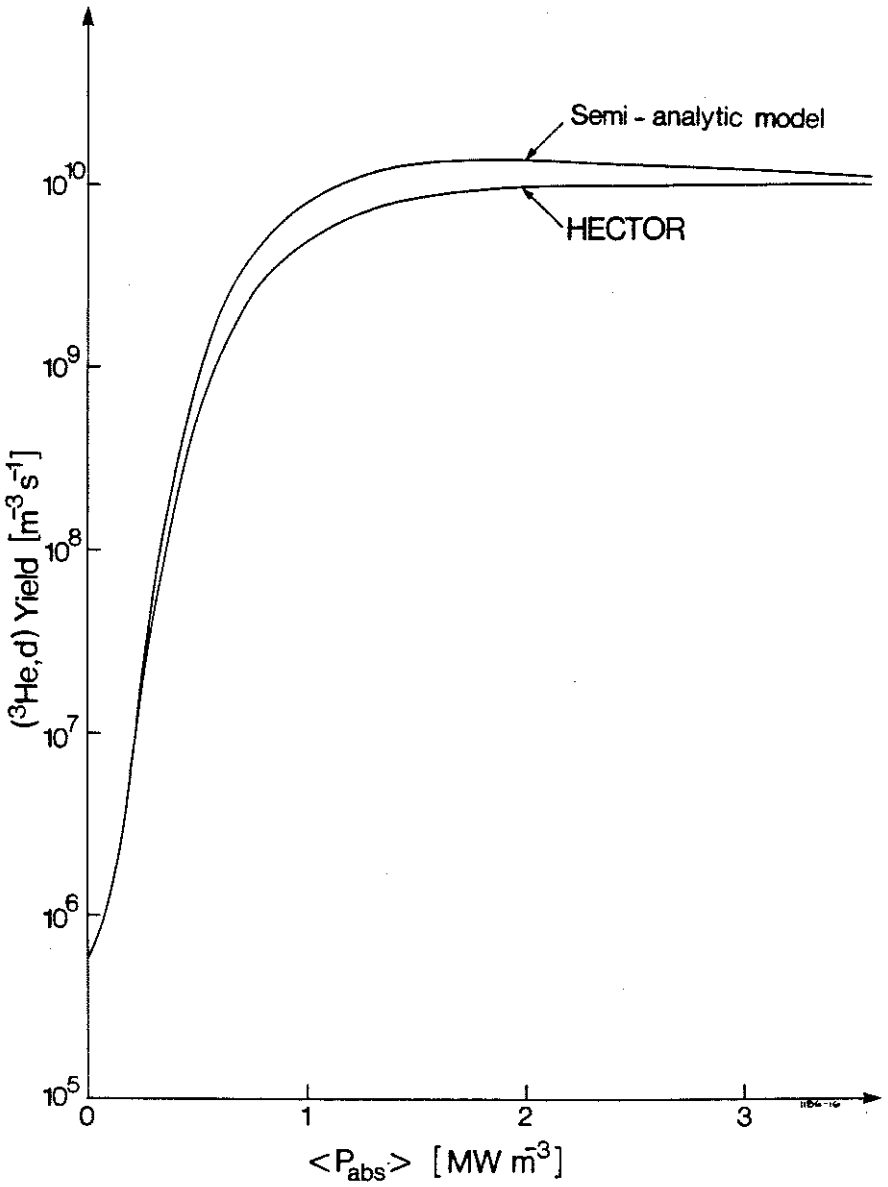

13. Comparison of the (^{3}He,d) yield calculated with the Fokker-Planck and HECTOR codes. Flat plasma and rf-wave field profiles were used to eliminate the finite orbit effects in HECTOR. The parameters for the calculation are I_p = 5 MA. B_ϕ = 3.4 T, T_e = 8 keV, $n_e = 5 \times 10^{19} m^{-3}$, Z_{eff} = 1.2.